Cancer Research

Forced Activation of Notch in Macrophages Represses Tumor Growth by Upregulating miR-125a and Disabling Tumor-Associated Macrophages

Jun-Long Zhao[1], Fei Huang[1], Fei He[2], Chun-Chen Gao[1], Shi-Qian Liang[1], Peng-Fei Ma[2], Guang-Ying Dong[1], Hua Han[1,2], and Hong-Yan Qin[1]

Abstract

Tumor-associated macrophages (TAM) contribute greatly to hallmarks of cancer. Notch blockade was shown to arrest TAM differentiation, but the precise role and underlying mechanisms require elucidation. In this study, we employed a transgenic mouse model in which the Notch1 intracellular domain (NIC) is activated conditionally to define the effects of active Notch1 signaling in macrophages. NIC overexpression had no effect on TAM differentiation, but it abrogated TAM function, leading to repressed growth of transplanted tumors. Macrophage miRNA profiling identified a novel downstream mediator of Notch signaling, miR-125a, which was upregulated through an RBP-J–binding site at the first intronic enhancer of the host gene *Spaca6A*. miR-125a functioned downstream of Notch signaling to reciprocally influence polarization of M1 and M2 macrophages by regulating factor inhibiting hypoxia inducible factor-1α and IRF4, respectively. Notably, macrophages transfected with miR-125a mimetics increased phagocytic activity and repressed tumor growth by remodeling the immune microenvironment. We also identified a positive feedback loop for miR-125a expression mediated by RYBP and YY1. Taken together, our results showed that Notch signaling not only supported the differentiation of TAM but also antagonized their protumorigenic function through miR-125a. Targeting this miRNA may reprogram macrophages in the tumor microenvironment and restore their antitumor potential. *Cancer Res; 76(6); 1403–15. ©2016 AACR.*

Introduction

Tumor-associated macrophages (TAM) play pivotal roles in tumor microenvironment to facilitate tumor growth and metastasis (1–3). TAMs inhibit antitumor immunity by recruiting myeloid-derived suppressor cells (MDSC) and regulatory T cells (Tregs), and by repressing $CD8^+$ cytotoxic T cells (1–3). TAMs are characterized by a molecular signature reminiscent of alternatively activated (M2) macrophages. These macrophages, with IL4-activated macrophages as a prototype, express higher levels of immunosuppressive cytokines such as TGFβ and IL10, together with arginase-1 (Arg-1), mannose receptor (MR) and other molecules involved in anti-inflammatory and/or tissue remodeling (4–6). TAMs also secret EGF and VEGF and other growth factors to promote cancer cell proliferation and tumor vascularization, respectively. In contrast to TAMs or M2 macrophages, lipopolysaccharide (LPS)- and IFNγ-stimulated macrophages or M1 macrophages upregulate IL12, inducible nitric oxide synthase (iNOS), and TNFα, accompanied by increased antigen presentation capacity. Macrophages with the M1 phenotype repress tumor growth through phagocytosis and enhanced antitumor immunity (1–3). Therefore, it is possible to reeducate TAMs to elicit antitumor activities, given that the regulation and mechanisms of macrophage polarization are established (7–9).

The Notch-RBP-J (recombination signal-binding protein Jκ) signaling pathway plays critical roles in cell fate specification and cell plasticity (10, 11). Notch signaling is involved in macrophage activation and polarization (12–19). Recently, Franklin and colleagues have demonstrated that Notch signal is required for TAMs differentiation in a mouse mammary tumor model (20). However, the role and mechanisms of Notch in TAMs after differentiation remain to be elucidated, although NF-κB, MAPK, STAT3, interferon regulatory factor (IRF) 8, and cylindromatosis (CYLD), as well as pyruvate dehydrogenase phosphatase 1 (Pdp1)-mediated mitochondrial metabolism reprogramming, have been implicated (17, 19, 21, 22).

miRNAs participate in myeloid differentiation and macrophage activation (23–25). miR-125a is enriched in myeloid progenitors but at low level in monocytes (25, 26), and is upregulated in M1 and downregulated in M2 macrophages (23, 24). miR-125a is involved in differential activation of

[1]State Key Laboratory of Cancer Biology, Department of Medical Genetics and Developmental Biology, Fourth Military Medical University, Xi'an, China. [2]Department of Hepatic Surgery, Xijing Hospital, Fourth Military Medical University, Xi'an, China.

Note: Supplementary data for this article are available at Cancer Research Online (http://cancerres.aacrjournals.org/).

J.-L. Zhao and F. Huang contributed equally to this article.

Corresponding Authors: Hong-Yan Qin, State Key Laboratory of Cancer Biology, Department of Medical Genetics and Developmental Biology, Fourth Military Medical University, Chang-Le Xi Street #169, Xi'an 710032, China. Phone: 8629-8477-4487; Fax: 8629-8324-6270; E-mail: hyqin@fmmu.edu.cn; and Hua Han, E-mail: huahan@fmmu.edu.cn

doi: 10.1158/0008-5472.CAN-15-2019

macrophages and other immune cells, as well as in myeloproliferative neoplasm (27–30). In this study, we show that forced Notch activation in macrophages by conditional overexpressing Notch intracellular domain (NIC) was sufficient to support TAM differentiation but abrogate TAM functions, most likely through miR-125a, leading to repressed tumor growth in mice.

Materials and Methods

Mice

Mice were maintained on C57BL/6 background in a specific pathogen–free (SPF) facility. *RBP-J*-floxed (*RBP-J^{f}*) mice (31) or *ROSA-Stop^{f}-NIC* transgenic mice (a gift from H.L. Li) were mated with *Lyz2-Cre* (#019096, Jackson Laboratory) or *Mx1-Cre* (provided by K. Rajewsky) mice to obtain mice with appropriate genotypes. *Mx1-Cre-RBP-J^{f}* mice were further injected intraperitoneally with 300 μg poly(I)-poly(C) (Sigma) to induce *RBP-J* gene disruption in bone marrow (inducible conditional RBP-J knockout, *RBP-J^{icKO}*; ref. 31). The *ROSA-Stop^{f}-NIC* transgenic mice contain a sequence encoding NIC (amino acids 1749-2293, lacking the C-terminal PEST domain) of the mouse Notch1 followed by a *IRES-GFP* cassette, which is inserted into the *GT(ROSA)26Sor* locus. Mice were genotyped with tail DNA by PCR using the primers listed in Supplementary Table S1. All animal experiments were approved by the Animal Experiment Administration Committee of the Fourth Military Medical University.

Lewis lung carcinoma (LLC) cells and B16F melanoma cells were purchased from the authenticated ATCC repository in 2014, and cell lines were tested by PCR for the absence of mycoplasma contamination and C57BL derivation during the experiment and injected subcutaneously on rear back of C57BL/6 mice. Tumor growth was monitored by measuring tumor length (*L*) and short (*S*) with a sliding caliper (tumor size $= L \times S^2 \times 0.51$). Mice were sacrificed 2 (B16F) or 4 (LLC) weeks after inoculation.

Cell culture

Bone marrow–derived macrophages (BMDM) were cultured from bone marrow monocytes as described previously (17). BMDMs were stimulated with LPS (50 ng/mL, Sigma) and IFNγ (20 ng/mL) or IL4 (20 ng/mL, PeproTech) for 24 hours. In some experiments, γ-secretase inhibitor IX (GSI, 30 μmol/L, Sigma) was included in the medium, with DMSO as a control. The transfection of BMDMs with synthetic miR-125a mimics or antisense oligonucleotides (ASO, Ribio) and siRNAs was performed by using Lipofectamine LTX (Invitrogen), according to the recommended protocol. The sequences of siRNAs for murine factor inhibiting hypoxia-inducible factor-1 α (*FIH1*), *IRF4*, Yin and Yang 1 (*YY1*), and *Notch1* are shown in Supplementary Table S1. RAW264.7 cells were cultured in DMEM supplemented with 10% FCS and 2 mmol/L L-glutamine and transfected with plasmids using Lipofectamine 2000 (Invitrogen).

Recombinant mD1R, which is composed of the DSL domain of mouse Dll1 and an arginine-glycine-aspartic acid (RGD) motif, was manufactured in *E. coli* (32). Wells of 12-well dishes were coated with 400 μL of mD1R (50 μg/mL) at 4°C overnight, with PBS as a control. BMDMs (5×10^5) were then seeded in the wells and cultured in the presence of LPS and IFNγ for 24 hours.

Allogenic T-cell stimulation assay was performed as described previously (17).

Immunofluorescence and flow cytometry

Cells were stained with antibodies listed in Supplementary Table S2, and observed under a laser scanning confocal microscope (FV-1000, Olympus). FACS analysis was performed using a FACSCalibur and FACSAriaII flow cytometer (BD Immunocytometry Systems). Data were analyzed with the FlowJo vX.0.6 software (FlowJo, LLC). Dead cells were excluded by propidium iodide (PI) staining.

Phagocytosis

L1210 murine leukemia cells (ATCC; 1×10^6 cells/mL) were labeled with carboxyfluorescein succinimidyl amino ester (CFSE; Dojindo Molecular Technologies, Inc.), and incubated with BMDMs (1×10^5 cells/mL) on coverslips at 37°C for 2 hours. After washing, samples were stained with anti-F4/80, and visualized under a fluorescence microscope (BX51, Olympus). The average number of engulfed L1210 cells per macrophage was calculated. The engulfment of bacteria by BMDMs was determined in a similar way by using *E. coli* BL21 transformed with an EGFP-expressing plasmid.

miRNA profiling

BMDMs from *RBP-J^{icKO}* and control mice were stimulated with LPS for 24 hours and used for miRNA expression profiling with an Agilent miRNA chip (Sanger miRBase v.12.0, 627 mouse miRNAs and 39 mouse viral miRNAs were represented) conducted by a commercial service (ShanghaiBio). The data were uploaded to Gene Expression Omnibus database (accession number GSE67364).

RT-PCR

Total RNA preparation, reverse transcription, and real-time PCR were performed as described, with *β-actin* or *U6* RNA (for miRNAs) as internal controls. Rapid amplification of cDNA ends (RACE) was performed using a SMARTer RACE cDNA Amplification Kit (Clontech). The PCR primers are shown in Supplementary Table S1.

Plasmids

The 3′-untranslated regions (UTR) of *IRF4*, *FIH1*, and RING1- and YY1-binding protein (*RYBP*) were amplified by PCR with a mouse cDNA library as a template. Point mutations were generated by PCR. Wild-type or mutant 3′-UTR fragments were inserted into pGL3-promoter (Promega) at the 3′ end of the luciferase gene to generate reporters (pGL3-IRF4, pGL3-HIF1, and pGL3-RYBP, respectively). The enhancer fragments of *pri-miR-125a* and *MR* genes were amplified by PCR with mouse genomic DNA as a template. These fragments and different truncations were inserted into pGL3-promoter to construct reporters (reporters 1–6 in Fig. 3A; pGL3-MR). A DNA fragment containing 4 × hypoxia responsive elements (*HRE*) was synthesized and inserted into pGL3-promoter to construct pGL3-HRE. pEF-BOS–NIC was as described previously (33). Full-length *PU.1*, *IRF4*, and *RYBP* cDNAs were amplified from a mouse cDNA library and inserted into pFlag-CMV2 to construct pFlag-PU.1, pFlag-IRF4, and pFlag-RYBP, respectively.

Reporter assay

HeLa cells were transfected with different combinations of reporters, expression vectors, and miRNA using Lipofectamine 2000, with a *Renilla* luciferase vector (phRL-TK, Promega) as an internal control. Cells were harvested 24 or 48 hours after the transfection, and luciferase activity was measured with Dual Luciferase Reporter Assay using a Gloma X 20/20 Luminometer (Promega).

Chromatin immunoprecipitation

Chromatin immunoprecipitation (ChIP) assays were performed by using a kit (Merck Millipore) according to the manufacturer's instructions using anti-RBP-J or anti-NIC antibody. Collected immune complexes were extracted and analyzed by PCR using the primers listed in Supplementary Table S1.

Western blot analysis

Whole cell lysates were extracted with the RIPA buffer (Beyotime). Protein concentration was determined with a BCA Protein Assay kit (Pierce). Samples were separated by SDS–PAGE, blotted onto polyvinylidenefluoride (PVDF) membranes and probed with primary and secondary antibodies (Supplementary Table S2). Membranes were developed with chemoluminescent reagents (Pierce).

NO production

BMDMs were cultured, and 50 μL culture supernatants were added to 50 μL Griess reagent I and 50 μL Griess reagent II (Beyotime). Absorbance was measured at 540 nm with a microplate reader.

Statistics

Images were imported into Image Pro Plus 5.1 software (Media Cybernetics Inc.) to quantify the densities of electrophoretic bands. Data were analyzed with Graph Pad Prism 5 software. Comparisons between groups were performed with unpaired Student *t* test or the paired *t* test. The results are expressed as the mean ± SD. $P < 0.05$ was considered significant.

Results

Forced activation of Notch signaling in macrophages abrogated TAM phenotypes

Notch1 was the dominant type of Notch receptors expressed in macrophages (Supplementary Fig. S1). Blocking Notch signaling by RBP-J disruption arrests TAM differentiation (20). To investigate the role of Notch signaling in TAMs after differentiation, we employed mice with a *NIC* transgene controlled by *Lyz2-Cre* (hereafter named as NIC^{cA}), which was expected to have sufficient TAM differentiation. No obvious abnormal myeloid development was noticed in NIC^{cA} mice (data not shown). In NIC^{cA} mice, the growth of subcutaneously inoculated LLC and B16F tumors was delayed significantly (Fig. 1A; Supplementary Fig. S2A). The number of TAMs showed no significant difference between the NIC^{cA} and control mice (Supplementary Fig. S2B, S3A, and S3B).

Although TAMs in NIC^{cA} mice expressed comparable levels of MHC II and VCAM-1, they expressed significantly lower level of MR (Supplementary Fig. S3A). qRT-PCR confirmed that several M1 markers increased and M2 markers decreased significantly in sorted TAMs from LLC tumors on NIC^{cA} mice (Fig. 1B), suggesting a loss of TAMs phenotypes. Consistently, $CD11b^{+}Ly6G^{+}$ MDSCs decreased whereas $CD8^{+}$ cytotoxic T cells increased in LLC tumors on NIC^{cA} mice (Fig. 1C; Supplementary Fig. S3C and S3D). Tumor vasculature also decreased remarkably (Fig. 1D). These results suggested that forced Notch activation in macrophages subverted TAMs phenotypes.

Identification of miR-125a as a downstream molecule of Notch signaling in macrophages

To identify molecules downstream to Notch signaling in regulating TAMs, we compared miRNA profiles between LPS-activated BMDMs derived from $RBP\text{-}J^{icKO}$ and control mice. Thirteen miRNAs exhibited differential expression between *RBP-J*-deficient and control macrophages (Fig. 2A). miR-125a was chosen for further investigation because several recent reports have highlighted its role(s) in macrophages (26–29).

We examined miR-125a expression in *RBP-J*–deficient ($RBP\text{-}J^{cKO}$) and *Notch*-activated (NIC^{cA}) macrophages stimulated with PBS (M0), LPS+IFNγ (M1), or IL4 (M2). The results showed that M1 polarization led to a significant upregulation of miR-125a whereas *RBP-J* deficiency led to its downregulation in macrophages (Fig. 2B). Constitutive Notch activation upregulated miR-125a, even in unstimulated macrophages (Fig. 2B). During the *in vitro* differentiation of monocytes into macrophages, the level of miR-125a increased steadily, in correlation with *RBP-J* and *Hey1* expression (Fig. 2C). Blocking Notch signaling by disrupting RBP-J or with GSI significantly suppressed miR-125a upregulation during macrophage differentiation *in vitro* (Fig. 2D; Supplementary Fig. S4).

To access the regulation of miR-125a expression by Notch signaling more specifically, we knocked down Notch1 expression in BMDMs using siRNA (Supplementary Fig. S5A). Notch1 knockdown resulted in attenuated M1 and strengthened M2 polarization of BMDMs (Supplementary Fig. S5B; ref. 17). Notch1 knockdown also reduced miR-125a expression during *in vitro* macrophage differentiation and activation (Fig. 2E; Supplementary Fig. S5C). Moreover, we activated Notch signaling in BMDMs with immobilized Notch ligand mD1R, and found that Notch activation resulted in upregulation of miR-125a (Fig. 2F; Supplementary Fig. S6). These data suggest that miR-125a is a downstream molecule of Notch signaling in macrophages.

Notch signaling directly transactivated the enhancer of *pri-miR-125a* through an RBP-J–binding site

The *pri-miR-125a* gene is located upstream to the sperm acrosome-associated protein *(Spaca) 6* gene (NC_000083.6; ref. 30). We performed 5′-RACE to determine the transcription starting site of *Spaca6/pri-miR-125a* using cDNA generated from BMDMs (Supplementary Fig. S7A). Sequencing the 5′-RACE-amplified fragment identified a novel exon (exon 1′) located 3.6 kb upstream to exon 1 of *Spaca6* (GenBank accession number KP893886), and an alternative splicing acceptor within exon 1 (Supplementary Fig. S7B and S7C). The first intron of *Spaca6A* contains three pri-miRNA genes including *pri-miR-99b*, *pri-let-7e*, and *pri-miR-125a*, and a putative

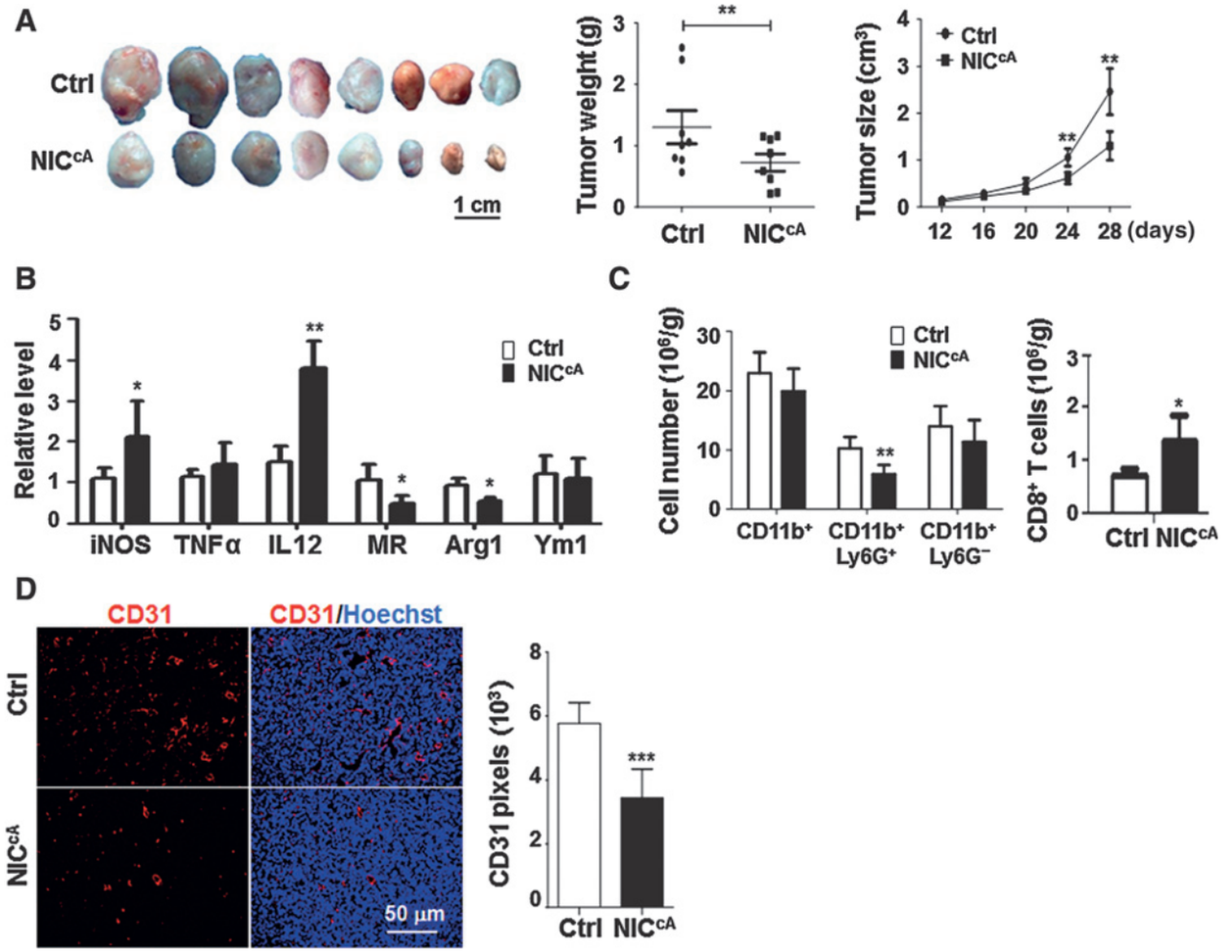

Figure 1.
Activation of Notch signaling in macrophages repressed tumor growth accompanied by diminished TAM phenotypes. A, *NIC*^{cA} and control (Ctrl) mice were inoculated subcutaneously with 5×10^6 of LLC cells. Tumors were dissected on day 28 after the inoculation, photographed, and tumor weights were measured. Tumor size was monitored from day 12 after the inoculation. B, $CD11b^+F4/80^+$ macrophages were sorted from the tumors, and the expression of the indicated molecules was determined by using qRT-PCR. C, single-cell suspensions were prepared from the tumors and analyzed by FACS after staining as indicated (Supplementary Fig. S3C and S3D). MDSCs ($CD11b^+Ly6G^+$) and cytotoxic T cells ($CD8^+$) were quantitatively compared. D, tumors were sectioned and stained with anti-CD31 followed by counterstaining with Hoechst. Pixels for CD31 were quantitatively compared. Bars, mean ± SD; *, $P < 0.05$; **, $P < 0.01$; ***, $P < 0.001$.

enhancer element containing recognition sites for YY1, MYB, Smad3, and RBP-J (Supplementary Fig. S8).

The full-length and truncated *pri-miR-125a* enhancer fragments were inserted into a pGL3-promoter to construct serial reporter genes (Fig. 3A, left). HeLa cells were cotransfected with pEF-BOS–NIC and different reporter constructs. All constructs with the RBP-J–binding site (reporters 1, 3, 4, and 5) were transactivated by NIC, and disruption of this site by mutagenesis (reporter 6) prevented NIC-mediated transactivation (Fig. 3A, right). ChIP assay indicated that, consistent with the miR-125a expression pattern, occupation of the RBP-J–binding site by RBP-J and NIC increased significantly on day 3 of BMDM differentiation *in vitro* (Fig. 3B). miR-99b was regulated coordinately by Notch signaling in BMDMs (Fig. 2E, 2F, 3C; Supplementary Fig. S5C). These data indicated that Notch signaling directly transactivated the enhancer of *pri-miR-125a* through the RBP-J–binding site.

miR-125a functioned downstream to Notch signaling to promote M1 and suppress M2 polarization

BMDMs from normal mice were transfected with miR-125a mimics or control oligonucleotides and stimulated with PBS, LPS+IFNγ, or IL4 for 24 hours. qRT-PCR showed that miR-125a upregulated the M1 markers iNOS, IL12, and TNFα, and downregulated the M2 marker MR in BMDMs (Fig. 4A). Moreover, transfection of miR-125a into BMDMs enhanced NO production (Fig. 4B). We also cocultured miR-125a–transfected BMDMs with allogenic naïve T cells, and found that miR-125a–overexpressing BMDMs promoted stronger T-cell proliferation (Fig. 4C). In addition, miR-125a–transfected BMDMs exhibited enhanced bacterial phagocytosis, consistent with enhanced M1 polarization (Supplementary Fig. S9). These results suggested that miR-125a promoted M1 and suppressed M2 polarization. In line with this finding, transfection of an ASO

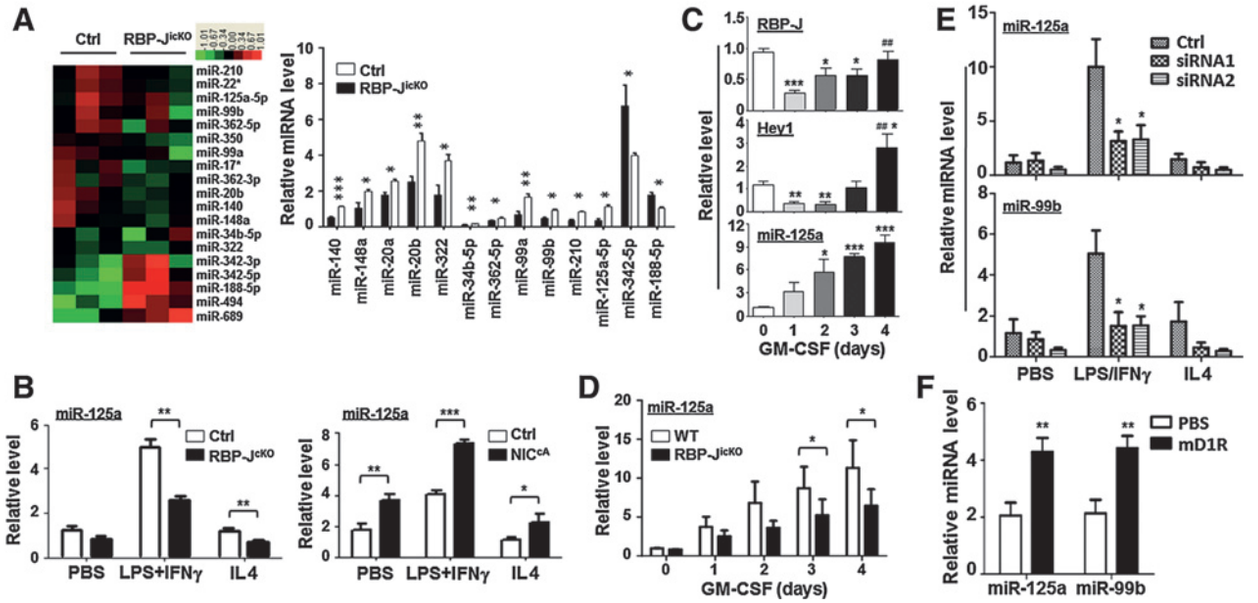

Figure 2.
miR-125a was a downstream molecule of Notch signaling in macrophages. A, BMDMs were prepared from *RBP-J*^{icKO} and control (Ctrl) mice and activated by LPS. miRNA expression was profiled by using microarray hybridization ($n = 3$) and was confirmed by using qRT-PCR ($n = 5$). B, BMDMs from *RBP-J*^{icKO} and Ctrl mice (left), or *NIC*^{cA} and control mice (right), were stimulated with PBS, LPS+IFNγ, or IL4. miR-125a expression was determined by using qRT-PCR ($n = 4$). C, monocytes from normal mice were cultured in the presence of GM-CSF for 4 days. RBP-J mRNA, Hey1 mRNA, and miR-125a were determined on days 0, 1, 2, 3, and 4 ($n = 3$). *, comparison with day 0; #, comparison with day 1. D, monocytes from *RBP-J*^{icKO} and control mice were induced to differentiate into BMDMs. miR-125a expression was detected using qRT-PCR ($n = 3$). E, BMDMs from normal mice were stimulated with PBS, LPS+IFNγ, or IL4 in the presence of control, siRNA1, or siRNA2 to *Notch1* (Supplementary Fig. S5A). The expression of miR-125a and miR-99b was determined by qRT-PCR. F, purified mD1R protein was coated on cultured dishes. BMDMs from normal mice were seeded and cultured in the presence of LPS+IFNγ. The expression of miR-125a and miR-99b was determined by qRT-PCR. Bars, mean ± SD; *, $P < 0.05$; ** and ##, $P < 0.01$; ***, $P < 0.001$.

of miR-125a downregulated M1 markers and upregulated MR (Fig. 4D).

In cultured BMDMs, Notch signaling enhanced M1 while suppressed M2 polarization (Supplementary Fig. S5B and S10; ref. 17). BMDMs were prepared from *RBP-J*^{cKO} and control mice and transfected with miR-125a mimics or control oligonucleotides, and stimulated with PBS, LPS+IFNγ, or IL4. Although *RBP-J* disruption downregulated iNOS and TNFα and upregulated MR, transfection of miR-125a reversed these changes (Fig. 4E). These results indicated that miR-125a acted downstream to Notch signaling to regulate macrophage polarization.

miR-125a–targeted FIH1 and IRF4 to enhance M1 and attenuate M2 polarization simultaneously

The 3′-UTRs of *FIH1* and *IRF4* are potential miR-125a targets (Supplementary Fig. S11A and S12A). BMDMs were transfected with miR-125a, and the expression of FIH1 and IRF4 was determined with Western blot analysis. FIH1 and IRF4 expression decreased significantly in BMDMs transfected with miR-125a (Fig. 5A). Reporter assay showed that miR-125a reduced luciferase activity in cells transfected with reporters containing the wild-type 3′-UTR of *FIH1* or *IRF4*, and disruption of the proximal seed sequence (302–309 bp) in the *FIH1* 3′-UTR or the unique seed sequence in the *IRF4* 3′-UTR abrogated this effect (Fig. 5B and 5C). These data suggested that miR-125a downregulated *FIH1* and *IRF4* in macrophages through their 3′-UTRs.

FIH1 suppresses HIF1α activity, which promotes M1 polarization through glycolysis and iNOS (34). Culturing BMDMs under hypoxia or knockdown of *FIH1* with siRNA upregulated iNOS in BMDMs (Supplementary Fig. S11B and S11C). Transfection with miR-125a enhanced pGL3-HRE transactivation mildly in BMDMs, suggesting that miR-125a enhanced HIF1α activity (Supplementary Fig. S11D). On the other hand, IRF4 enhances M2 polarization (35, 36). IRF4 knockdown downregulated the M2 marker MR (Supplementary Fig. S12B). IRF4 binds to PU.1, and there are four PU.1-binding sites in or near the MR promoter (37, 38; Supplementary Fig. S12C). ChIP assay confirmed that IRF4 could be recruited to the PU.1 site in the first intron of the *MR* gene (Supplementary Fig. S12C), and transactivated the *MR* enhancer reporter (pGL3-MR) in RAW264.7 cells (Supplementary Fig. S12D), which was dependent on PU.1 in NIH3T3 cells (Supplementary Fig. S12E). Consistently, transfection of miR-125a suppressed pGL3-MR transactivation in RAW264.7 cells (Supplementary Fig. S12F).

To further evaluate the contribution of FIH1 and IRF4 to miR-125a–mediated macrophage polarization, we cotransfected BMDMs with a miR-125a ASO and siRNA targeting *FIH1* or *IRF4*. The miR-125a ASO downregulated M1 markers IL12, iNOS, and TNFα, and upregulated the M2 marker MR. FIH1 knockdown partially rescued the effect of the miR-125a ASO by increasing IL12, iNOS, and TNFα expression (Fig. 5D). On the other hand, IRF4 knockdown reduced MR expression and nearly reversed miR-125a ASO-mediated MR upregulation (Fig. 5E). These results suggested that miR-125a promoted

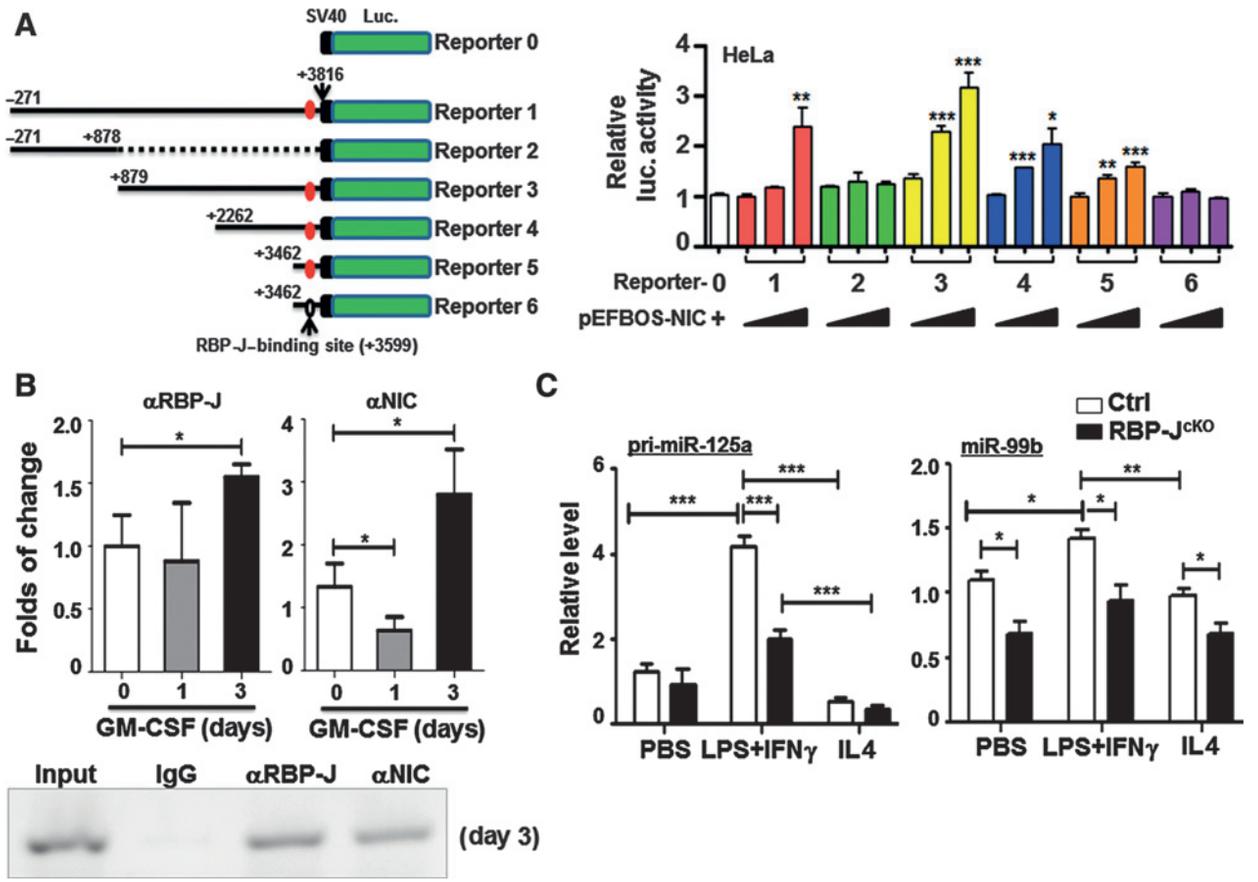

Figure 3.
Notch signaling directly regulated the enhancer of *pri-miR-125a*. A, reporter assay. HeLa cells were transfected with reporters containing different truncated or mutated *pri-miR-125a* enhancer, together with different amounts (0, 50, or 100 ng) of pEF-BOS–NIC. Relative luciferase activity was determined 48 hours after the transfection ($n = 6$). B, normal bone marrow monocytes were cultured with GM-CSF and collected on days 0, 1, and 3 for ChIP with IgG, anti-RBP-J, or anti-NIC antibody. The precipitated chromatin DNA was amplified by PCR and analyzed on a 2% agarose gel (bottom, for day 3) and qPCR (top; $n = 4$). C, *pri-miR-125a* (left) and miR-99b (right) were determined in differentially stimulated BMDMs derived from RBP-J^{cKO} and control (Ctrl) mice ($n = 4$). Bars, mean ± SD; *, $P < 0.05$; **, $P < 0.01$; ***, $P < 0.001$.

M1 and suppressed M2 polarization simultaneously through FIH1-HIF1α pathway and IRF4, respectively.

Macrophages overexpressing miR-125a exhibited strong antitumor activity

The expression of miR-125a was upregulated in sorted TAMs overexpressing NIC (Fig. 6A). We transduced BMDMs with a lentivirus overexpressing miR-125a and EGFP, with lentivirus expressing EGFP only as a control. These BMDMs were mixed with LLC cells and inoculated in normal mice. miR-125a-overexpressing macrophages strongly repressed tumor growth (Fig. 6B). FACS analysis of tumoral macrophages indicated that in the EGFP$^+$ compartment, macrophages overexpressing miR-125a expressed a higher level of iNOS and a lower level of MR, suggesting that they were M1-polarized (Fig. 6C). Interestingly, in the EGFP$^-$ compartment most, if not all, host-derived macrophages were also M1-polarized (Fig. 6C, right). The expression of *pri-miR-125a*, *iNOS*, *TNFα*, and *IL12* increased whereas the expression of *MR*, *IL10*, and *TGFβ* decreased significantly in tumors containing miR-125a-overexpressing macrophages (Fig. 6D). In addition, the number of CD11b$^+$Ly6G$^+$ MDSCs decreased in tumors and spleens, whereas CD8$^+$ T cells increased in tumors and lymph nodes, of mice bearing tumors containing miR-125a–overexpressing macrophages (Fig. 6E). These results suggested that macrophages overexpressing miR-125a skewed the immune microenvironment of the tumors into an antitumor state. Moreover, BMDMs transfected with miR-125a exhibited stronger phagocytic activity to L1210 leukemia cells *in vitro*, suggesting that miR-125a enhanced direct antitumor activities of macrophages (Fig. 6F).

miR-125a amplified its own expression through RYBP

RYBP mRNA was another predicted potential target of miR-125a (Supplementary Fig. S13A). RYBP binds YY1 to suppress transcription (39, 40). Two YY1 recognition sites exist in the *pri-miR-125a* enhancer (Supplementary Fig. S7 and S8). Therefore, it is likely that miR-125a augments its own expression in macrophages through a negative feedback loop composed of miR-125a–RYBP/YY1–*pri-miR-125a* enhancer. BMDMs were transfected with miR-125a. Western blot analysis showed that miR-125a efficiently downregulated RYBP expression (Fig. 7A). Consistently, reporter assay indicated that miR-125a suppressed

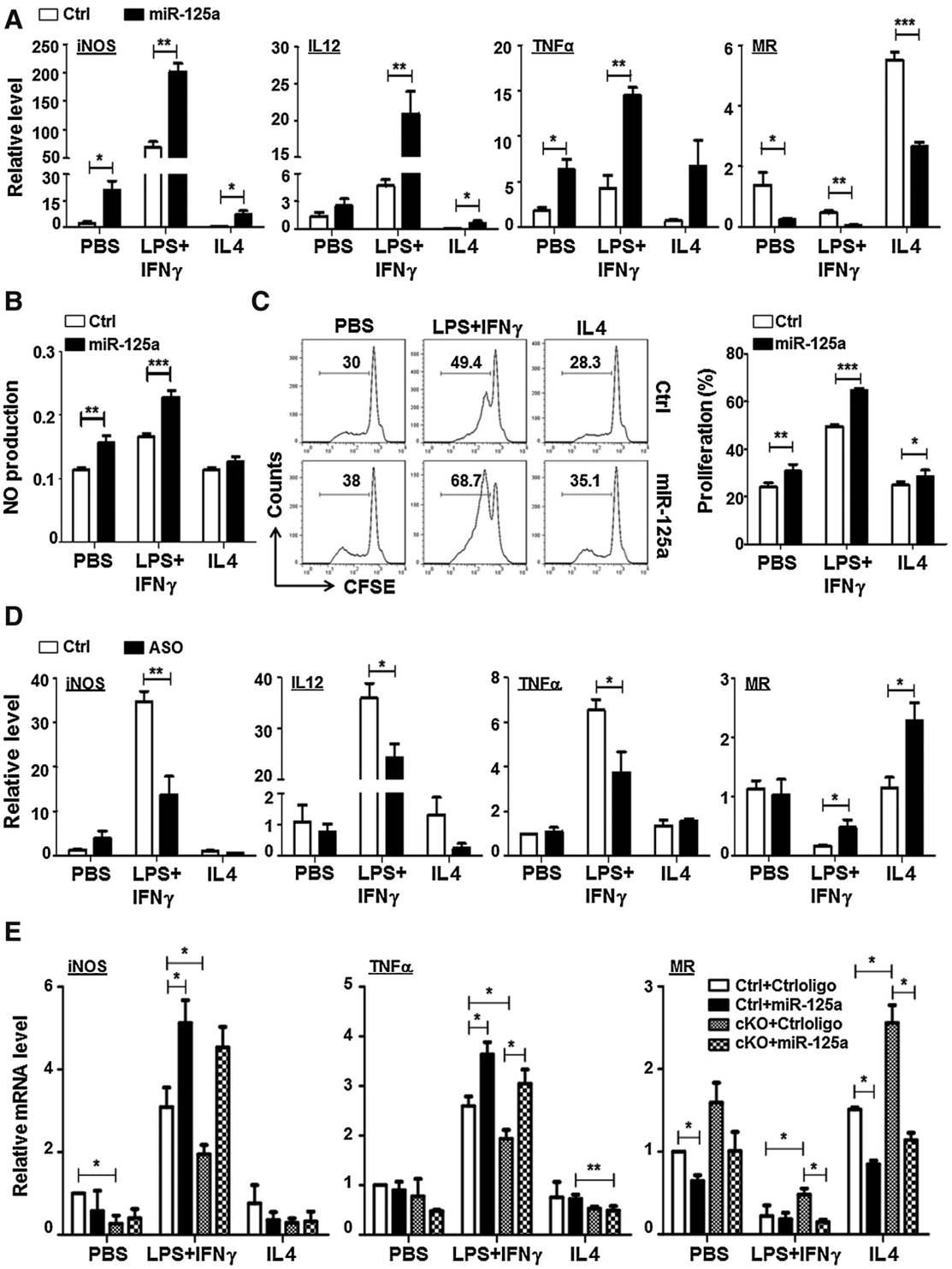

Figure 4.

miR-125a regulated macrophage polarization downstream to Notch signaling. A, BMDMs were transfected with miR-125a mimics or control oligonucleotides and stimulated with PBS, LPS+IFNγ or IL4. The expression of iNOS, IL12, TNFα, and MR was determined by using qRT-PCR ($n = 3$). B, NO production was measured in BMDMs in A. C, BMDMs in A were irradiated and cocultured with CFSE-loaded allogeneic T cells for 24 hours. T-cell proliferation was determined by FACS ($n = 6$). D, BMDMs from wild-type mice were transfected with miR-125a ASO or control and stimulated with PBS, LPS+IFNγ or IL4. The expression of iNOS, IL12, TNFα and MR was determined with qRT-PCR ($n = 3$). E, BMDMs derived from *RBP-J*^{cKO} and control (Ctrl) mice were transfected with miR-125a mimics or control oligonucleotides (Ctrloligo) and treated with PBS, LPS+IFNγ, or IL4. The expression of iNOS, TNFα, and MR mRNA was determined with qRT-PCR ($n = 3$). Bars, mean ± SD; *, $P < 0.05$; **, $P < 0.01$; ***, $P < 0.001$.

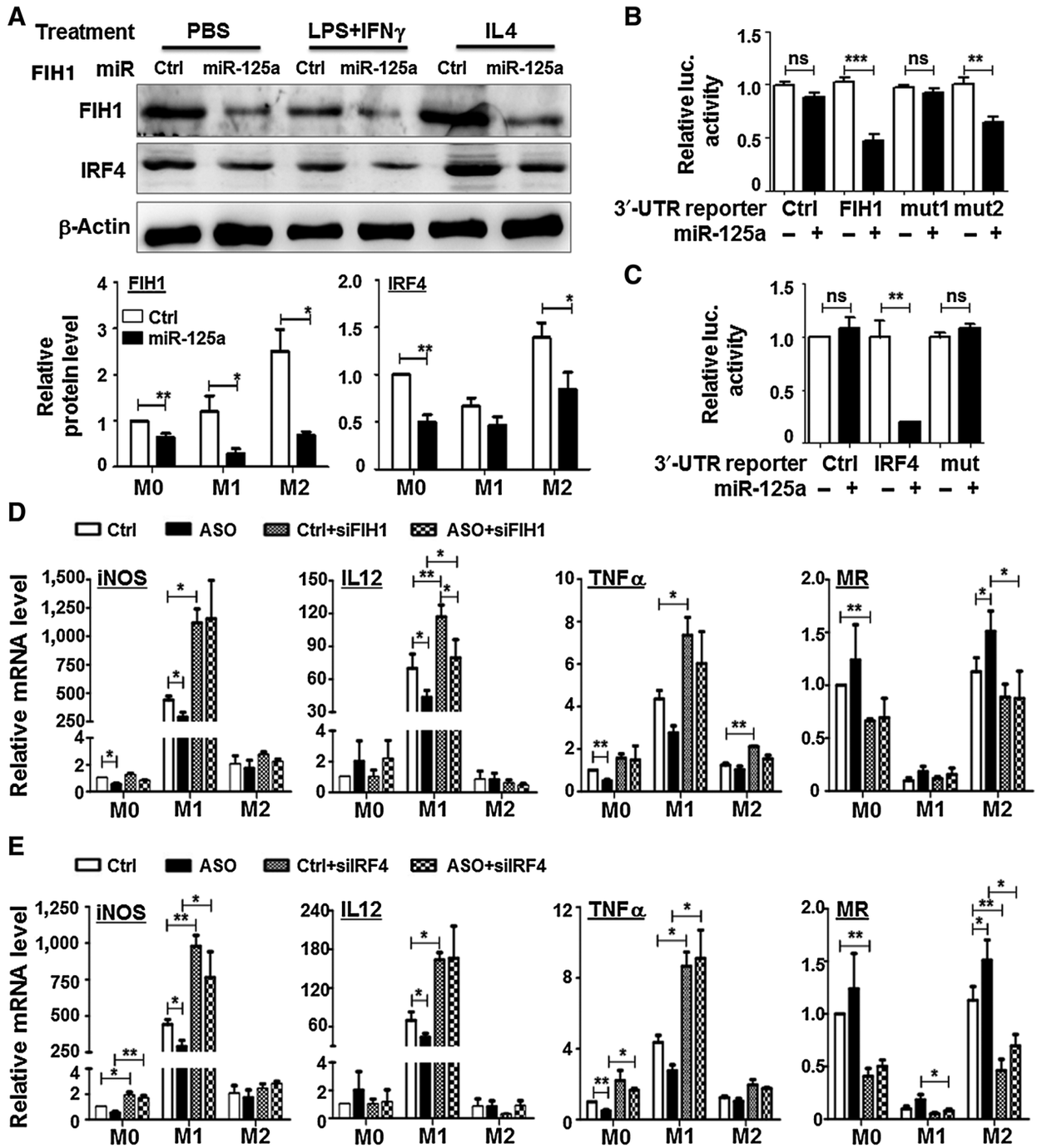

Figure 5.
miR-125a promoted M1 and suppressed M2 polarization by targeting FIH1 and IRF4, respectively. A, normal BMDMs were transfected with miR-125a mimics or control and stimulated with PBS, LPS+IFNγ or IL4, followed by Western blot analysis 48 hours after the transfection. The relative FIH1 and IRF4 protein levels were quantitatively compared (lower; $n = 4$). B and C, HeLa cells were transfected with miR-125a mimics or control, together with reporters containing wild-type and mutant 3′-UTRs of FIH1 (B) or IRF4 (C). Luciferase activity was determined 24 hours after the transfection ($n = 4$). D and E, normal BMDMs were transfected with miR-125a ASO or control, together with siFIH1 (D) or siIRF4 (E). Cells were stimulated with PBS (M0), LPS+IFNγ (M1) or IL4 (M2), and the expression of iNOS, IL12, TNFα, and MR was determined by qRT-PCR ($n = 3$). Bars, mean ± SD; *, $P < 0.05$; **, $P < 0.01$; ***, $P < 0.001$; ns, not significant.

a reporter encoding the 3′-UTR of RYBP mRNA (Fig. 7B). RYBP overexpression significantly downregulated miR-125a and miR-99b in RAW264.7 cells (Supplementary Fig. S13B), and knockdown of YY1 with siRNA reversed the downregulation of miR-125a resulted from ectopic RYBP overexpression (Fig. 7C). Reporter assay showed that RYBP overexpression suppressed

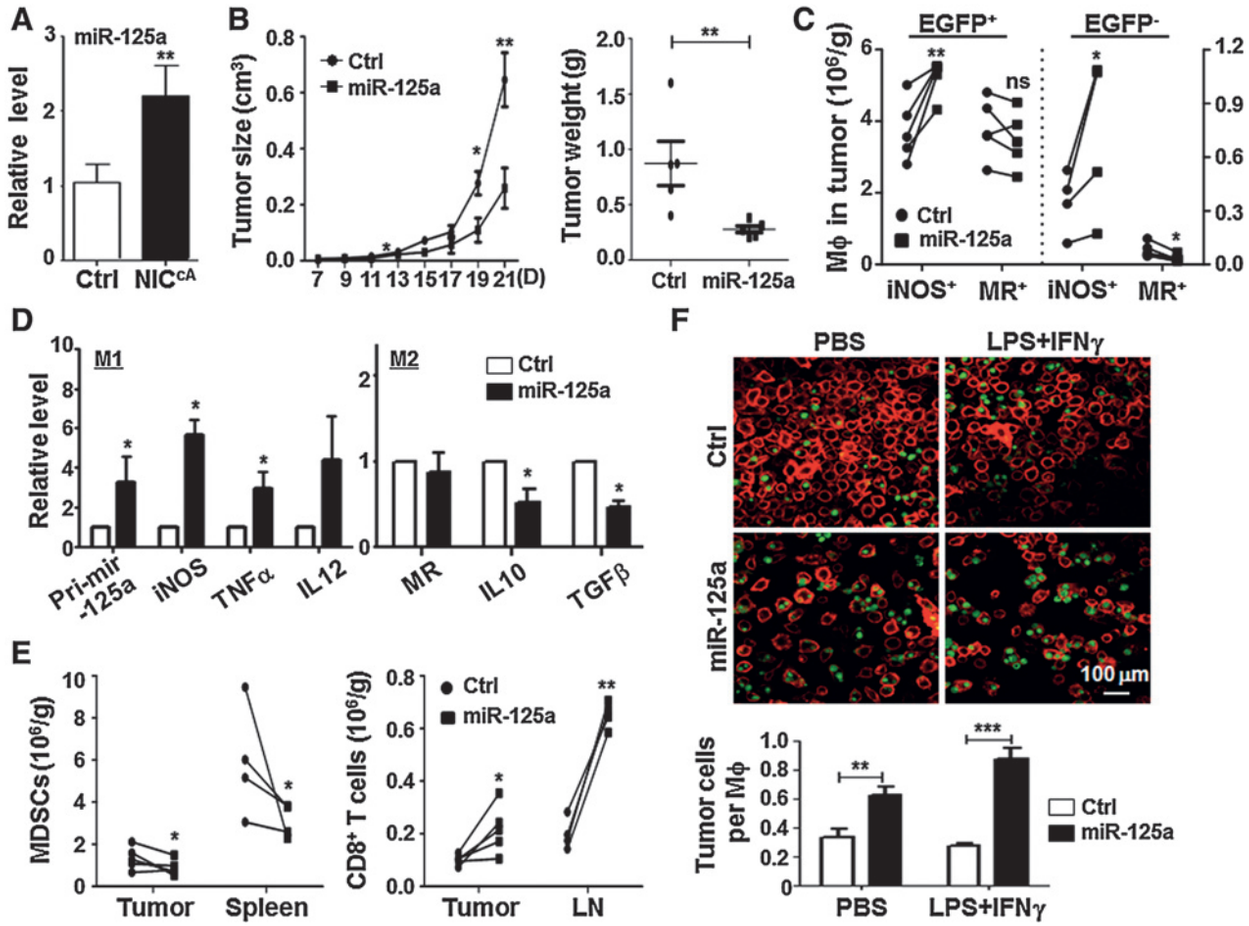

Figure 6.

Macrophages overexpressing miR-125a exhibited strong antitumor activity. A, TAMs were sorted from tumors in Fig. 1A, and miR-125a expression was determined by qRT-PCR ($n = 5$). B, normal BMDMs were transduced with a lentivirus overexpressing miR-125a and EGFP or EGFP only (Ctrl). Cells (1×10^6) were mixed with LLC cells (5×10^6) and injected subcutaneously in normal mice. Tumor sizes were monitored on the indicated days (left), and their weights were measured on day 21 after the inoculation (right; $n = 5$). C, macrophages ($CD11b^+F4/80^+$) in tumors in B were analyzed by FACS after staining for cytoplasmic iNOS and MR. The numbers of $iNOS^+$ and MR^+ macrophages in the $EGFP^+$ and $EGFP^-$ compartments were compared. D, total RNA was extracted from the tumors described in B, and the *pri-miR-125a, iNOS, TNFα, IL12, MR, IL10*, and *TGFβ* were determined by qRT-PCR ($n = 5$). E, tumor-infiltrating cells, splenocytes, and lymph node (LN) cells from the mice described in B were analyzed by FACS after staining with anti-CD11b and anti-Ly6G or anti-CD3 and anti-CD8. The numbers of MDSCs ($CD11b^+Ly6G^+$, left) and $CD8^+$ T cells ($CD3^+CD8^+$, right) were compared ($n = 4$). F, normal BMDMs transfected with miR-125a mimics or control (Ctrl) were stimulated with PBS or LPS+IFNγ. Cells (1×10^5) were cocultured with CFSE-labeled L1210 cells (1×10^6) for 2 hours and observed under a fluorescence microscope (top). The numbers of tumor cells engulfed per macrophage were compared (bottom; $n = 6$). Bars, mean ± SD; *, $P < 0.05$; **, $P < 0.01$; ***, $P < 0.001$; ns, not significant.

transactivation of a reporter containing the full length *pri-miR-125a* enhancer fragment (reporter 1 in Fig. 3A), and this suppression was reversed by knockdown of YY1 with siRNA (Fig. 7D), suggesting that RYBP inhibited miR-125a expression through YY1. In BMDMs transfected with miR-125a, the expression of both *pri-miR-125a* and miR-99b was enhanced (Fig. 7E). These data suggested that miR-125a could positively regulate its enhancer to augment its expression in macrophages.

Discussion

A novel mechanism mediating the regulation of TAMs by Notch signaling

Conditional deletion of *RBP-J* abrogated $CD11c^+$ TAMs while maintained $MHCII^{hi}CD11b^{hi}$ macrophages in the MMTV-PyMT mammary tumor model, suggesting that Notch signaling is specifically required for the differentiation of TAMs (20). In this study, to overcome this *RBP-J* disruption-mediated developmental arrest of TAMs, we employed conditionally activated *NIC* transgenic mice. FACS analyses of macrophages in tumors suggested that TAMs existed in a similar number as in the control. This provided us a chance to evaluate the consequence of Notch activation on TAMs phenotypes. Our results indicated that TAMs with forced Notch activation exhibited M1 phenotype and antitumor activity. Therefore, in addition to supporting TAMs differentiation, Notch signaling represses the tumor-promoting activity of TAMs (Supplementary Fig. S14). However, due to the limitations of the cancer model and gene-modified mice used in this study, more efforts are required to clarify other potential

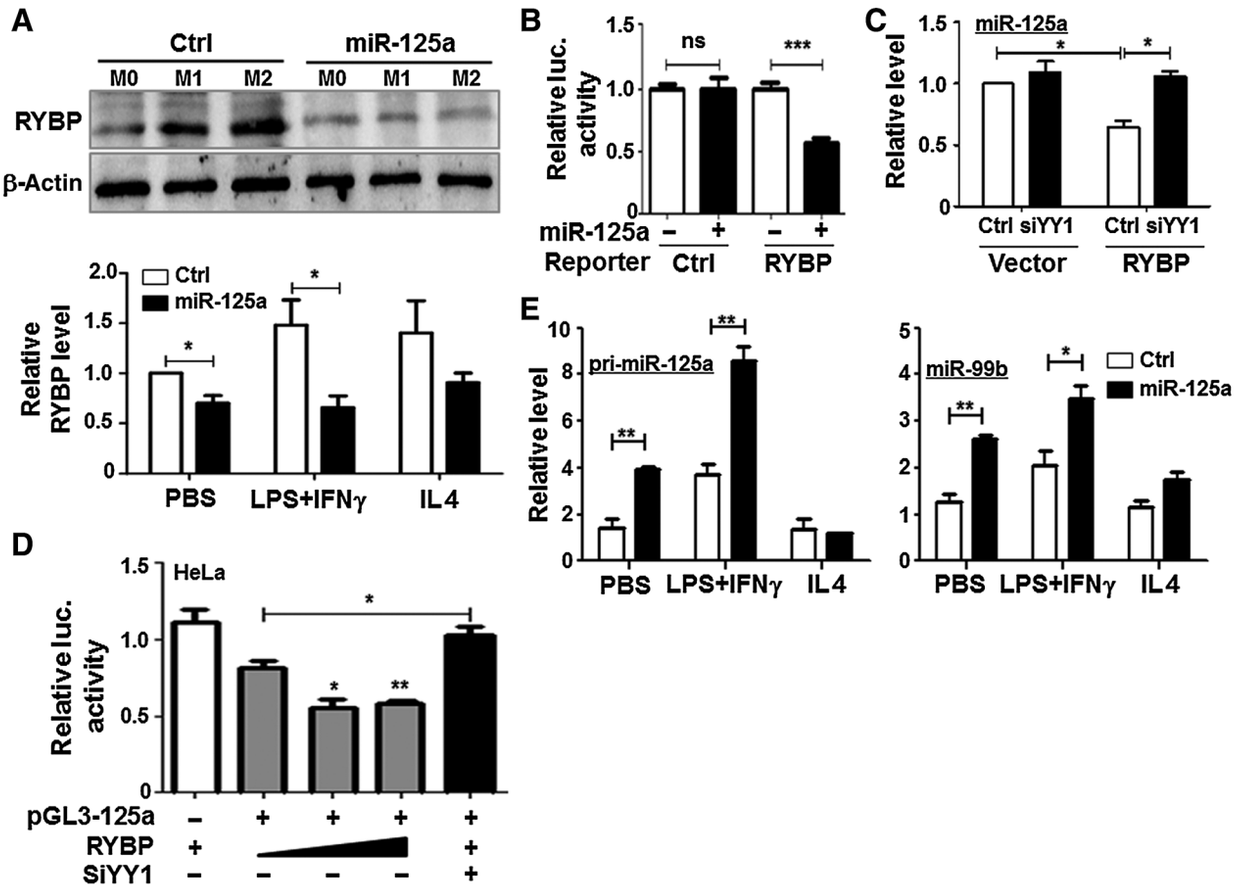

Figure 7.

Self-amplification of miR-125a expression through RYBP/YY1. A, normal BMDMs transfected with miR-125a mimics or control were stimulated with PBS, LPS+IFNγ, or IL4. RYBP expression was determined by Western blot analysis 48 hours after the transfection (top), and the relative RYBP protein levels were quantitatively compared (bottom; $n = 3$). B, HeLa cells were transfected with miR-125a mimics or control, together with reporters containing wild-type and mutant 3′-UTRs of RYBP. Luciferase activity was determined 24 hours after the transfection ($n = 6$). C, RAW264.7 cells were transfected with pFlag-RYBP or control, plus siYY1 or control, and miR-125a was determined by qRT-PCR ($n = 3$). D, HeLa cells were transfected with the reporter 1 in Fig. 3A, together with siYY1 and pFlag-RYBP. Luciferase activity was determined 48 hours after the transfection ($n = 3$). E, BMDMs transfected with miR-125a mimic or control (Ctrl) were stimulated with PBS, LPS+IFNγ, or IL4 for 24 hours. The expression of pri-miR-125a and miR-99b was determined by qRT-PCR 48 hours after the transfection ($n = 3$). Bars, mean ± SD; *, $P < 0.05$; **, $P < 0.01$; ***, $P < 0.001$; ns, not significant.

mechanisms underlying the discrepancy between the phenotypes of CD11c-Cre–mediated RBP-J cKO (20) and Lyz2-Cre–mediated NIC^{cA} mice (this study). First, the consequence of NIC overexpression may not be exactly compatible with the phenotype of RBP-J disruption due to the existence of noncanonical Notch signaling that is independent of RBP-J. Second, different Cre transgenic mice were used in the two studies, which might impact differentially on other myeloid cells such as neutrophils in addition to macrophages. Third, LLC cells used in this study might exert different influence on macrophages from that of the MMTV-PyMT mammary cancer cells used in the RBP-J cKO study. Finally and most importantly, it could not be excluded that subcutaneously inoculated LLC tumors might contain different subsets of macrophages from the MMTV-PyMT mammary tumors. How Notch signaling regulates these different subsets of macrophages remains an open question.

Notch signaling modulates the activation of macrophages by targeting a variety of downstream molecules (12–19, 41). Moreover, macrophages, regardless of their embryonic or bone marrow origins, proliferate *in situ* at sites of inflammation, such as cancer (4, 42). This raises the question of how polarized macrophages maintain their phenotypes. miRNAs are a class of noncoding RNAs involved in epigenetic regulation and macrophage activation (43). We identified miR-125a as a novel target of canonical Notch signaling in macrophages. As a downstream molecule of Notch signaling that regulates macrophage activation, miR-125a has several important properties. First, it enhances M1 polarization and suppresses M2 polarization simultaneously. We have previously shown that disrupting Notch signaling reduces M1 and increases M2 macrophage polarization, even in the presence of M1 inducers (17). We and others have also identified IRF8, CYLD, and SOCS3 as downstream targets of Notch signaling in the

regulation of macrophage activation (17–19). However, these models consider that M1 polarization is a result of Notch activation and M2 polarization represents a "default" state. In this study, we showed that Notch signaling led to the upregulation of miR-125a, which may actively enhance M1 and suppress M2 polarization through FIH1 and IRF4, respectively (Supplementary Fig. S14). Second, Foldi and colleagues have shown that the Notch pathway amplifies its own signaling during macrophage activation (44). miR-125a may participate in the self-amplification of Notch signaling strength during macrophage activation by upregulating its own expression through suppressing RYBP, which functions as a transcriptional repressor of the *Spaca6A/pri-miR-125a* enhancer via interaction with YY1. Last but not least, it has been widely accepted that macrophages proliferate *in situ* in solid tumors to elicit long-lasting protumor activities (4, 42). Notch-miR-125a signaling may play a role in the epigenetic memory associated with the immune-suppressing and tumor-promoting capacities of TAMs. Further experiments are required to clarify this possibility.

miR-125a expression has been shown to be higher in M2 macrophages and to promote their polarization by targeting KLF13 (26, 27). However, in the current study, we showed that miR-125a was induced in M1 macrophages after LPS+IFNγ stimulation and that miR-125a overexpression promoted M1 polarization by targeting FIH1 while inhibiting M2 polarization by targeting IRF4. This inconsistency might be a consequence of different experimental conditions employed during the induction of macrophage activation and polarization. In contrast with granulocyte-macrophage colony-stimulating factor (GM-CSF) and M-CSF, which have been previously used to induce M1 and M2 macrophage polarization, respectively (26), we employed LPS+IFNγ or IL4 stimulation. Other studies have also shown that miR-125a expression is upregulated after stimulation with LPS, consistent with our observation and other reports (24). In addition, it should be noted that FIH1 inhibits both HIF1α and HIF2α, which play opposite roles in macrophage polarization (34). Therefore, it cannot be formally excluded that under specific conditions, miR-125a might also enhance M2 macrophage activation. A recent report has unveiled other activities of miR-125a (30), also prompting further investigations.

Notch-miR-125a signaling might also be involved in monocyte-to-macrophage differentiation *in vitro* (Fig. 2C; Supplementary Fig. S1A). Schroeder and Just have reported that Notch signaling promotes myeloid differentiation through RBP-J (45). However, RBP-J KO does not significantly change the number of myeloid colony-forming units in bone marrow (31). Notch signaling has been implicated in various myeloid malignancies (46). Disruption of this signaling pathway leads to myeloproliferation in mice (47, 48). Additional studies are required to elucidate the mechanism by which Notch signaling regulates myeloid development.

Education of macrophages to elicit antitumor activities using miR-125a

TAMs have been widely recognized as a major tumor-promoting population during tumor initiation, growth, invasion, and metastasis (1–3). Macrophage depletion shows tumor-repressive effects in several experimental systems (7, 8). However, as an important cell population in innate immunity, macrophages may also elicit antitumor activities (7). It has been speculated that TAMs can be "educated" to perform antitumor functions, if their phenotypes are reversible. Indeed, blocking CSF1R signaling in TAMs leads to the conversion of M2-like macrophages to M1-like macrophages (49). Moreover, a recent study has shown that low-dose irradiation of tumors induces massive increases in M1 macrophages in the tumors (9). The results of this study indicated that miR-125a–overexpressing macrophages exhibited strong antitumor activities. These macrophages possessed M1 characteristics and enhanced phagocytosis of tumor cells. More importantly, miR-125–overexpressing macrophages exhibited M1-polarized characteristics with increased secretion of TNFα and IL12. The immune microenvironment molded by miR-125a–overexpressing macrophages had higher levels of TNFα and IL12 and lower levels of IL10 and TGFβ, which mediate M1 and M2 polarization, respectively (1, 2, 7). This cytokine milieu would polarize newly recruited macrophages into M1 directly or indirectly, accompanied by enhanced $CD8^+$ T-cell infiltration and diminished MDSC recruitment. Moreover, these macrophages proliferated in tumors while retaining their M1 characteristics, which strengthened their antitumor activities. Therefore, our findings may facilitate the development a new therapeutic strategy for tumors based on Notch- or miR-125a–modified macrophages in the future.

Disclosure of Potential Conflicts of Interest

No potential conflicts of interest were disclosed.

Authors' Contributions

Conception and design: H. Han, H.-Y. Qin
Development of methodology: J.-L. Zhao, F. Huang
Acquisition of data (provided animals, acquired and managed patients, provided facilities, etc.): J.-L. Zhao, F. Huang, F. He, C.-C. Gao, S.-Q. Liang, P.-F. Ma, G.-Y. Dong
Analysis and interpretation of data (e.g., statistical analysis, biostatistics, computational analysis): J.-L. Zhao, F. Huang, F. He, S.-Q. Liang, P.-F. Ma, G.-Y. Dong, H. Han, H.-Y. Qin
Writing, review, and/or revision of the manuscript: H. Han, H.-Y. Qin
Administrative, technical, or material support (i.e., reporting or organizing data, constructing databases): J.-L. Zhao, F. Huang, H. Han, H.-Y. Qin
Study supervision: H. Han, H.-Y. Qin

Acknowledgments

The authors thank H.L. Li and K. Rajewsky for mice. The study was performed at the Graduates Innovation Center of the Fourth Military Medical University.

Grant Support

This work was supported by grants from Ministry of Science and Technology (2015CB553702) and National Natural Science Foundation of China (31130019, 31371474, 31570878, 81530018, 31301127, 81170963, 31071291).

The costs of publication of this article were defrayed in part by the payment of page charges. This article must therefore be hereby marked *advertisement* in accordance with 18 U.S.C. Section 1734 solely to indicate this fact.

Received July 24, 2015; revised December 18, 2015; accepted January 4, 2016; published OnlineFirst January 12, 2016.

References

1. Biswas SK, Allavena P, Mantovani A. Tumor-associated macrophages: functional diversity, clinical significance, and open questions. Semin Immunopathol 2013;35:585–600.
2. De Palma M, Lewis CE. Macrophage regulation of tumor responses to anticancer therapies. Cancer Cell 2013;23:277–86.
3. Epelman S, Lavine KJ, Randolph GJ. Origin and functions of tissue macrophages. Immunity 2014;41:21–35.
4. Noy R, Pollard JW. Tumor-associated macrophages: from mechanisms to therapy. Immunity 2014;41:49–61.
5. Medina-Echeverz J, Aranda F, Berraondo P. Myeloid-derived cells are key targets of tumor immunotherapy. Oncoimmunology 2014;3: e28398.
6. Pollard JW. Trophic macrophages in development and disease. Nat Rev Immunol 2009;9:259–70.
7. Qian BZ, Pollard JW. Macrophage diversity enhances tumor progression and metastasis. Cell 2010;141:39–51.
8. Wynn TA, Chawla A, Pollard JW. Macrophage biology in development, homeostasis and disease. Nature 2013;496:445–55.
9. Klug F, Prakash H, Huber PE, Seibel T, Bender N, Halama N, et al. Low-dose irradiation programs macrophage differentiation to an iNOS(+)/M1 phenotype that orchestrates effective T cell immunotherapy. Cancer Cell 2013;24:589–602.
10. Artavanis-Tsakonas S, Rand MD, Lake RJ. Notch signaling: cell fate control and signal integration in development. Science 1999;284: 770–76.
11. Kopan R, Ilagan MX. The canonical Notch signaling pathway: unfolding the activation mechanism. Cell 2009;137:216–33.
12. Monsalve E, Perez MA, Rubio A, Ruiz-Hidalgo MJ, Baladrón V, García-Ramírez JJ, et al. Notch-1 up-regulation and signaling following macrophage activation modulates gene expression patterns known to affect antigen-presenting capacity and cytotoxic activity. J Immunol 2006;176: 5362–73.
13. Grandbarbe L, Michelucci A, Heurtaux T, Hemmer K, Morga E, Heuschling P. Notch signaling modulates the activation of microglial cells. Glia 2007;55:1519–30.
14. Hu X, Chung AY, Wu I, Foldi J, Chen J, Ji JD, et al. Integrated regulation of Toll-like receptor responses by Notch and interferon-gamma pathways. Immunity 2008;29:691–703.
15. Palaga T, Buranaruk C, Rengpipat S, Fauq AH, Golde TE, Kaufmann SH, et al. Notch signaling is activated by TLR stimulation and regulates macrophage functions. Eur J Immunol 2008;38:174–83.
16. Outtz HH, Wu JK, Wang X, Kitajewski J. Notch1 deficiency results in decreased inflammation during wound healing and regulates vascular endothelial growth factor receptor-1 and inflammatory cytokine expression in macrophages. J Immunol 2010;185:4363–73.
17. Wang YC, He F, Feng F, Liu XW, Dong GY, Qin HY, et al. Notch signaling determines the M1 versus M2 polarization of macrophages in antitumor immune responses. Cancer Res 2010;70: 4840–9.
18. Zhang W, Xu W, Xiong S. Blockade of Notch1 signaling alleviates murine lupus via blunting macrophage activation and M2b polarization. J Immunol 2010;184:6465–78.
19. Xu H, Zhu J, Smith S, Foldi J, Zhao B, Chung AY, et al. Notch-RBP-J signaling regulates the transcription factor IRF8 to promote inflammatory macrophage polarization. Nat Immunol 2012;13: 642–50.
20. Franklin RA, Liao W, Sarkar A, Kim MV, Bivona MR, Liu K, et al. The cellular and molecular origin of tumor-associated macrophages. Science 2014;344:921–5.
21. Xu J, Chi F, Guo T, Punj V, Lee WNP, French SW, et al. NOTCH reprograms mitochondrial metabolism for proinflammatory macrophage activation. J Clin Invest 2015;125:1579–90.
22. He F, Guo FC, Li Z, Yu HC, Ma PF, Zhao JL, et al. Myeloid-specific disruption of recombination signal binding protein Jkappa ameliorates hepatic fibrosis by attenuating inflammation through cylindromatosis in mice. Hepatology 2015;61:303–14.
23. O'Connell RM, Rao DS, Baltimore D. microRNA regulation of inflammatory responses. Annu Rev Immunol 2012;30: 295–312.
24. Graff JW, Dickson AM, Clay G, McCaffrey AP, Wilson ME. Identifying functional microRNAs in macrophages with polarized phenotypes. J Biol Chem 2012;287:21816–25.
25. Mildner A, Chapnik E, Manor O, Yona S, Kim KW, Aychek T, et al. Mononuclear phagocyte miRNome analysis identifies miR-142 as critical regulator of murine dendritic cell homeostasis. Blood 2013;121: 1016–27.
26. Guo S, Bai H, Megyola CM, Halene S, Krause DS, Scadden DT, et al. Complex oncogene dependence in microRNA-125a-induced myeloproliferative neoplasms. Proc Natl Acad Sci USA 2012;109: 16636–41.
27. Zhao X, Tang Y, Qu B, Cui H, Wang S, Wang L, et al. MicroRNA-125a contributes to elevated inflammatory chemokine RANTES levels via targeting KLF13 in systemic lupus erythematosus. Arthritis Rheum 2010;62: 3425–35.
28. Kim SW, Ramasamy K, Bouamar H, Lin AP, Jiang D, Aguiar RC. MicroRNAs miR-125a and miR-125b constitutively activate the NF-kappaB pathway by targeting the tumor necrosis factor alpha-induced protein 3 (TNFAIP3, A20). Proc Natl Acad Sci USA 2012; 109:7865–70.
29. Banerjee S, Cui H, Xie N, Tan Z, Yang S, Icyuz M, et al. miR-125a-5p regulates differential activation of macrophages and inflammation. J Biol Chem 2013;288:35428–36.
30. Pan W, Zhu S, Dai D, Liu Z, Li D, Li B, et al. MiR-125a targets effector programs to stabilize Treg-mediated immune homeostasis. Nat Commun 2015;6:7096.
31. Han H, Tanigaki K, Yamamoto N, Kuroda K, Yoshimoto M, Nakahata T, et al. Inducible gene knockout of transcription factor recombination signal binding protein-J reveals its essential role in T versus B lineage decision. Int Immunol 2002;14:637–45.
32. Tian DM, Liang L, Zhao XC, Zheng MH, Cao XL, Qin HY, et al. Endothelium-targeted Delta-like 1 promotes hematopoietic stem cell expansion *ex vivo* and engraftment in hematopoietic tissues *in vivo*. Stem Cell Res 2013;11:693–706.
33. Hu YY, Fu LA, Li SZ, Chen Y, Li JC, Han J, et al. Hif-1alpha and Hif-2alpha differentially regulate Notch signaling through competitive interaction with the intracellular domain of Notch receptors in glioma stem cells. Cancer Lett 2014;349:67–76.
34. Brune B, Dehne N, Grossmann N, Jung M, Namgaladze D, Schmid T, et al. Redox control of inflammation in macrophages. Antioxid Redox Signal 2013;19:595–637.
35. Negishi H, Ohba Y, Yanai H, Takaoka A, Honma K, Yui K, et al. Negative regulation of Toll-like-receptor signaling by IRF-4. Proc Natl Acad Sci USA 2005;102:15989–94.
36. Satoh T, Takeuchi O, Vandenbon A, Yasuda K, Tanaka Y, Kumagai Y, et al. The Jmjd3-Irf4 axis regulates M2 macrophage polarization and host responses against helminth infection. Nat Immunol 2010;11: 936–44.
37. Marecki S, Atchison ML, Fenton MJ. Differential expression and distinct functions of IFN regulatory factor 4 and IFN consensus sequence binding protein in macrophages. J Immunol 1999;163: 2713–22.
38. McKercher SR, Lombardo CR, Bobkov A, Jia X, Assa-Munt N. Identification of a PU.1-IRF4 protein interaction surface predicted by chemical exchange line broadening. Proc Natl Acad Sci USA 2003; 100:511–6.
39. Garcia E, Marcos-Gutierrez C, del Mar Lorente M, Moreno JC, Vidal M. RYBP, a new repressor protein that interacts with components of the mammalian Polycomb complex, and with the transcription factor YY1. EMBO J 1999;18:3404–18.
40. Deng Z, Cao P, Wan MM, Sui G. Yin Yang 1: a multifaceted protein beyond a transcription factor. Transcription 2010;1:81–4.
41. Zhou D, Huang C, Lin Z, Zhan S, Kong L, Fang C, et al. Macrophage polarization and function with emphasis on the evolving roles of coordinated regulation of cellular signaling pathways. Cell Signal 2014;26:192–7.
42. Ginhoux F, Jung S. Monocytes and macrophages: developmental pathways and tissue homeostasis. Nat Rev Immunol 2014;14: 392–404.

43. Liu G, Abraham E. MicroRNAs in immune response and macrophage polarization. Arterioscler Thromb Vasc Biol 2013;33:170–7.
44. Foldi J, Chung AY, Xu H, Zhu J, Outtz HH, Kitajewski J, et al. Autoamplification of Notch signaling in macrophages by TLR-induced and RBP-J-dependent induction of Jagged1. J Immunol 2010;185:5023–31.
45. Schroeder T, Just U. Notch signalling via RBP-J promotes myeloid differentiation. EMBO J 2000;19:2558–68.
46. Yin DD, Fan FY, Hu XB, Hou LH, Zhang XP, Liu L, et al. Notch signaling inhibits the growth of the human chronic myeloid leukemia cell line K562. Leuk Res 2009;33:109–14.
47. Kim YW, Koo BK, Jeong HW, Yoon MJ, Song R, Shin J, et al. Defective Notch activation in microenvironment leads to myeloproliferative disease. Blood 2008;112:4628–38.
48. Wang L, Zhang H, Rodriguez S, Cao L, Parish J, Mumaw C, et al. Notch-dependent repression of miR-155 in the bone marrow niche regulates hematopoiesis in an NF-kappaB-dependent manner. Cell Stem Cell 2014;15:51–65.
49. Strachan DC, Ruffell B, Oei Y, Bissell MJ, Coussens LM, Pryer N, et al. CSF1R inhibition delays cervical and mammary tumor growth in murine models by attenuating the turnover of tumor-associated macrophages and enhancing infiltration by CD8 T cells. Oncoimmunology 2013;2:e26968.